Reaction efficiency of diffusion-controlled processes on finite, planar arrays

Roberto A. Garza-López
Department of Chemistry, Pomona College, Claremont, California 91711

John J. Kozak
Department of Chemistry, Iowa State University, Ames, Iowa 50011
(Received 5 August 1993; revised manuscript received 12 October 1993)

In this paper we investigate the reaction efficiency of diffusion-controlled processes on finite, planar arrays having physical or chemical receptors. This problem translates into the statistical-mechanical one of examining the geometrical factors affecting the trapping of a random walker on small lattices of dimension $d=2$, having N sites and average valency $\bar{\nu}$. Extensive calculations of the site-specific average walk length $\langle n \rangle$ before trapping, a measure of the efficiency of the underlying diffusion-reaction process, have been carried out on triangular, square-planar, hexagonal, and Penrose platelets for $N=16$ and $N=48$. From the variety of distinct lattices considered, and the data generated, three general conclusions can be drawn. First, for fixed N, the smaller the number N_b of vertices defining the boundary of the finite lattice under consideration, the smaller the value of the (overall) average walk length $\langle \bar{n} \rangle$ of the random walker before trapping. Second, for fixed N and fixed N_b, the smaller the value of the (overall) root-mean-square distance $(\bar{r}^2)^{1/2}$ of the N lattice sites relative to the center of the array, the smaller the value of $\langle \bar{n} \rangle$. Third, for fixed $\{N, N_b, (\bar{r}^2)^{1/2}\}$, $\langle \bar{n} \rangle$ decreases with an increase in the (overall) average valency $\bar{\nu}$ of lattice sites comprising the array. Thus there are similarities but also real and significant differences in the conclusions drawn here in studying stochastic processes taking place on small, finite lattices of arbitrary shape and those found in studying nearest-neighbor random walks on infinite, periodic lattices of unit cells characterized by a given (N,d,ν). We comment on these and on the possible relevance of this work to one aspect of morphogenesis, viz., predicting the morphologies assumed by small platelets when growth is optimized with respect to (chemical or physical) signal processing at receptor sites.

PACS number(s): 05.40.+j

I. INTRODUCTION

Owing to physical and/or chemical interactions, the defining constituents (atoms, molecules) of a surface are often organized, at least locally, into well-defined constellations having hexagonal, square-planar, or triangular symmetry. Although such geometrical structures can persist globally, on extended length scales it is more usual to find that surfaces are broken up into domains, each of finite extent, with the boundaries separating these domains, and their intersections, defining a latticelike array which itself may be regular, quasiregular, or random. For finite systems, either isolated domains of definite symmetry or patterns formed from the juxtaposition of m domains, one anticipates that the overall shape and encompassing boundary of a finite array will be of critical importance in influencing processes dependent on the geometrical organization of the system.

As one example of such a process, consider a molecule diffusing in free space and colliding with a surface. Assume that the molecule is sufficiently entrained by surface forces that there results a reduction in dimensionality of its diffusion space from $d=3$ to $d=2$, and that in its subsequent random motion the molecule is sterically constrained to follow the boundary lines separating adjacent atoms or molecules in a given domain (or the boundary lines separating adjacent domains). If at some point in its trajectory the molecule becomes permanently immobilized, either because of physical binding at a site or because an irreversible reaction has occurred at that site, then, qualitatively, this sequence of events is descriptive of many diffusion-reaction processes in biology, chemistry, and physics.

The above surface-diffusion problem can be translated into a lattice-statistical one which, to our knowledge, has not been studied systematically. The objective is to calculate the mean walk length $\langle n \rangle$ of molecule constrained to move (randomly) along sterically allowed pathways on a structured surface until immobilized at a receptor or target site. Although the literature dealing with various aspects of the random-walk problem is vast [1], the important feature of the present work is that we consider explicitly processes taking place on domains of *finite* extent having boundaries of *arbitrary* shape. Thus, in formulating and then solving (here numerically) the stochastic problem of determining the first moment $\langle n \rangle$ of the underlying distribution function of the process, a quantity related to the mean relaxation time τ and hence a measure of the reaction efficiency, the simplifying feature of periodic boundary conditions *cannot* be imposed.

Recall that in the classic studies of Montroll and Weiss on nearest-neighbor random walks on an infinite, *periodic* lattice of unit cells [2], the mean walk length $\langle n \rangle$ was completely determined once the dimensionality d, the

number N of sites, and the connectivity (or valency) ν of the underlying unit cell were specified. For the class of $d=2$ problems considered here, we shall find, not unexpectedly, a more subtle dependence of $\langle n \rangle$ on the lattice parameters N and ν and a further, pronounced dependence on the shape of the domain. In particular, for a given setting of N_b, the number of lattice points defining the boundary of the domain, we shall show that trends in the values of $\langle n \rangle$ calculated for a wide variety of finite lattices of given bilateral symmetry but of various shapes can be systematically organized in terms of the (overall) root-mean-square distance $(\bar{r}^2)^{1/2}$ of the N lattice sites from the center of the array.

II. FORMULATION

We wish to calculate the mean walk length $\langle n \rangle$ before the trapping of a particle (atom or molecule) diffusing randomly on a series of $(d=2)$-dimensional finite lattices characterized by different geometries and connectivities (valencies). The calculational procedure used here, which leads to numerically exact values of $\langle n \rangle$, is based on the theory of finite Markov processes [3]. The interpretation of the results generated rests on the relationship between the moments of the underlying distribution function for the process being described and solutions of the stochastic master equation for the problem [4], where

$$\frac{d\rho_i(t)}{dt} = -\sum_{j=1}^{N} G_{ij}\rho_j(t) \quad (i=1,2,\ldots,N) \tag{1}$$

for the specific lattice geometry and initial conditions being considered. In Eq. (1), $\rho_i(t)$ is the probability that a diffusing particle has reached site i at time t on a lattice of N sites. The G_{ij} is an $N\times N$ matrix whose elements are the transition probabilities between neighboring sites on the lattice; in particular, one assigns unit relaxation rates between any two neighboring sites (i,j), so that $G_{ij}=-1$ for $i\neq j$ and $G_{ii}=\sum_{k\neq i}G_{ki}=\nu_i$, where k indexes the nearest-neighbor sites (only) and ν_i is the valency of site i of the lattice. Solutions of the above system (1) of linear equations are of the form

$$\rho_i(t) = \sum_{m=1}^{N} a_{im}\exp(-\lambda_m t) , \tag{2}$$

where a_{im} are coefficients determined by the initial conditions and the λ_m are the eigenvalues of the **G** matrix. For N large, it can be shown [5] that the reciprocal of the smallest eigenvalue λ_1 of the **G** matrix is related to the first moment (the mean walk length $\langle n \rangle$) of the probability distribution function defining the process, viz.,

$$\langle n \rangle = \bar{\nu}\lambda_1^{-1} , \tag{3}$$

where here $\bar{\nu}$ is the average valency of the (lattice) system. Thus calculations of the average walk length $\langle n \rangle$ before trapping provide a measure of the efficiency of the underlying diffusion-reaction process, and it is this relationship which is exploited in interpreting the results reported in this paper.

Before proceeding, we note that *all* lattices studied in this paper are characterized by a common (unit) distance l $(\equiv 1)$ separating lattice points. That is, although we shall consider lattices of different $\{N,N_b,\nu_i\}$, where N is the total number of lattice sites i, N_b is the number of boundary sites, ν_i is the (site-specific) valency, and

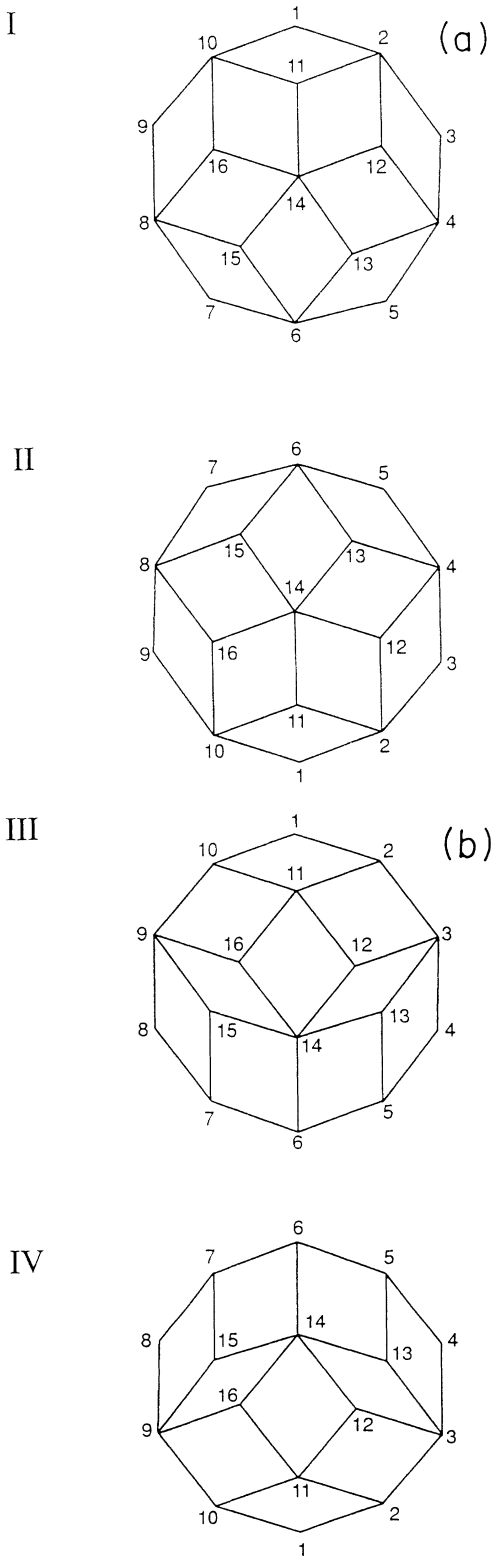

FIG. 1. (a) Lattice characteristics $\{N,N_b,(\bar{r}^2)^{1/2},\bar{\nu}\}$ $=\{16,10,1.395\,984,3.125\}$. (b) Lattice characteristics: $\{N,N_b(\bar{r}^2)^{1/2},\bar{\nu}\}=\{16,10,1.512\,821,3.125\}$.

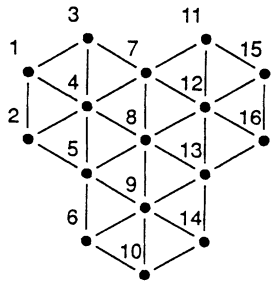

(a)

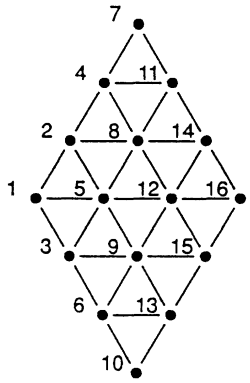

(b)

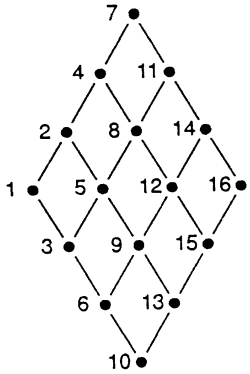

(c)

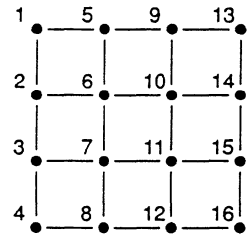

(d)

FIG. 2. (a) Lattice characteristics: $\{N,N_b,(\bar{r}^2)^{1/2},\bar{\nu}\}=\{16,12,1.500\,000,4.125\}$. (b) Lattice characteristics: $\{N,N_b,(\bar{r}^2)^{1/2},\bar{\nu}\}=\{16,12,1.581\,139,4.125\}$. (c) Lattice characteristics: $\{N,N_b,(\bar{r}^2)^{1/2},\bar{\nu}\}=\{16,12,1.581\,139,3.000\}$. (d) Lattice characteristics: $\{N,N_b,(\bar{r}^2)^{1/2},\bar{\nu}\}=\{16,12,1.581\,139,3.000\}$.

TABLE I. Lattice characteristics and stochastic results: Figs. 1–3.

Lattice	N	N_b	$(\bar{r}^2)^{1/2}$	$\langle\bar{n}\rangle$	$\bar{\nu}$	A
Fig. 1(a)	16	10	1.395 984	23.325 121	3.125	7.694
Fig. 1(b)	16	10	1.512 821	23.697 968	3.125	7.694
Fig. 2(a)	16	12	1.500 000	24.527 863	4.125	7.794
Fig. 2(b)	16	12	1.581 139	25.194 569	4.125	7.794
Fig. 2(c)	16	12	1.581 139	25.257 143	3.000	9.000
Fig. 2(d)	16	12	1.581 139	25.257 143	3.000	9.000
Fig. 3	16	14	1.802 776	27.989 569	2.375	10.392

different overall geometries, we impose here a common metric l for all lattices. The number of microlattices characterized by a given setting of $\{N,N_b,\nu_i\}$ obviously escalates with increase in N; the lattices studied here have been designed to allow the separate influence of the variables $\{N,N_b,\nu_i\}$ on the dynamics [as described by Eqs. (2) and (3)] to be disentangled.

Consider first the structures diagramed in Figs. 1–3. Each of the structures is characterized by the triplet $(d,N,N_b)=(2,16,N_b)$. In particular, $N_b=10$ for the two Penrose platelets diagrammed in Fig. 1, $N_b=12$ for the figures shown in Fig. 2, and $N_b=14$ for the single figure displayed in Fig. 3.

Consider next the lattices diagrammed in Figs. 4–7. The first series (Fig. 4) is characterized by $(d,N,N_b)=(2,48,22)$, the second series (Fig. 5) by $(d,N,N_b)=(2,48,24)$, the third series (Fig. 6) by $(d,N,N_b)=(2,48,30)$, and the fourth series (Fig. 7) by $(d,N,N_b)=(2,48,34)$.

Finally, the simple "ladder" diagram $(d,N,N_b)=(2,48,48)$, not displayed, has also been studied, along with the more structured lattices displayed in Figs. 8 and 9.

III. DISCUSSION

Calculation of the site-specific $\langle n\rangle_i$ for the lattices considered in this study [6] reveals that, consistent with one's "intuition," the farther the receptor site (trap) is removed from the "center" of a given lattice, the larger the value of $\langle n\rangle_i$. This result already stands in contrast to

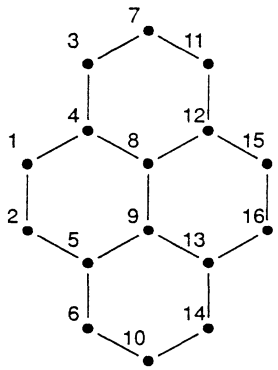

FIG. 3. Lattice characteristics: $\{N,N_b,(\bar{r}^2)^{1/2},\bar{\nu}\}=\{16,14,1.802\,776,2.375\}$.

the one that pertains when nearest-neighbor random walks on an infinite, periodic lattice of unit cells are studied. In the latter case, owing to the imposition of periodic boundary conditions, the value calculated for $\langle n \rangle_i$ is invariant regardless of the positioning of the trap. This distinction provides the first indication that one's intuition might fail in trying to interpret the results reported here on finite lattices, if that intuition were based solely on results obtained in earlier lattice-statistical studies in which a unit cell was identified and periodic boundary conditions were imposed or, more specifically, if one's understanding were rooted only in the analytical studies of Montroll and Weiss [2]. Montroll proved, for $(d=2)$-dimensional random walks on periodic lattices characterized by a uniform valency v, that

$$\langle n \rangle = \frac{N}{N-1}\{A_1 N \ln N + A_2 N + A_3 + A_4/N\} , \quad (4)$$

where the coefficients $\{A_1, A_2, A_3, A_4\}$ for hexagonal $(v=3)$, square-planar $(v=4)$, and triangular $(v=6)$ lattices are given, respectively, by

$$\{A_1, A_2, A_3\} = \{3\sqrt{3}/4\pi, +0.066\,206\,698, -0.254\,227\,9\} \quad (v=3) , \quad (5)$$

$$\{A_1, A_2, A_3, A_4\} = \{1/\pi, +0.195\,056\,166, -0.116\,964\,81, -0.051\,456\,50\} \quad (v=4) , \quad (6)$$

$$\{A_1, A_2, A_3\} = \{\sqrt{3}/2\pi, +0.235\,214\,021, -0.251\,407\,596\} \quad (v=6) . \quad (7)$$

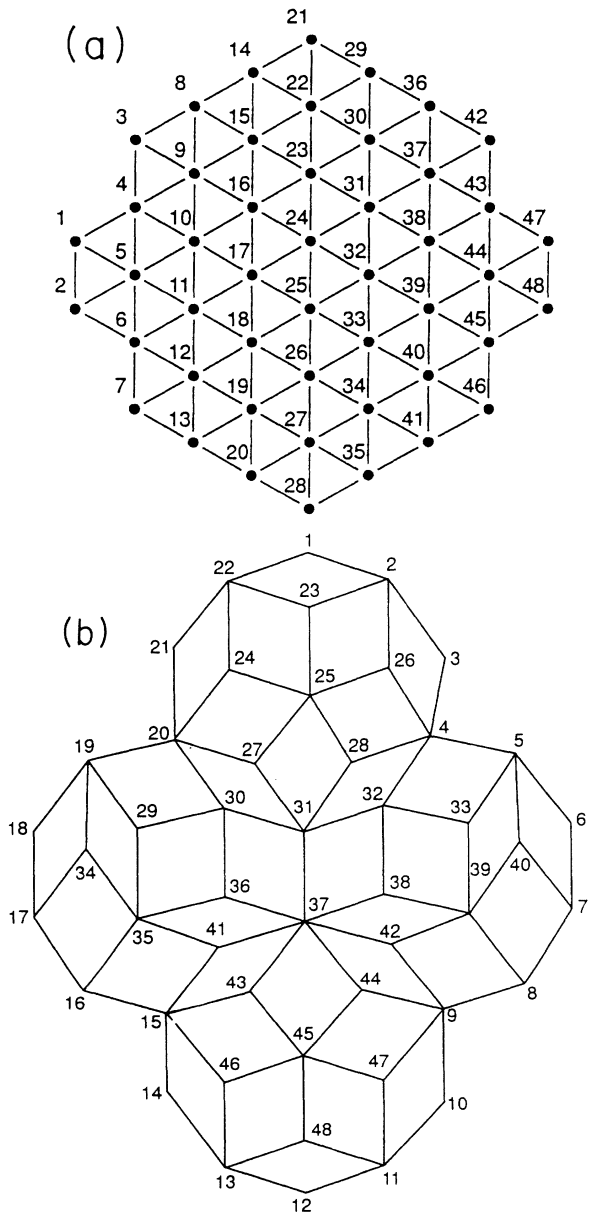

FIG. 4. (a) Lattice characteristics: $\{N, N_b, (\bar{r}^2)^{1/2}, \bar{v}\} = \{48, 22, 2.565\,801, 4.979\}$. (b) Lattice characteristics: $\{N, N_b, (\bar{r}^2)^{1/2}, \bar{v}\} = \{48, 22, 2.576\,481, 3.458\}$.

den Hollander and Kasteleyn [7] showed analytically that the term A_4 for the square-planar case $(v=4)$ was, in fact, $A_4 = +0.484\,065\,704$, a result confirmed numerically in Ref. [8], where estimates of A_4 for the cases $v=3$ and 6 were also given. However, the main point is that for large lattices the behavior of $\langle n \rangle$ is dominated by the first terms in the expression (4) which, in turn, means that, for fixed v, $\langle n \rangle$ increases with an increase in the total number N of lattice points and that, for fixed N, $\langle n \rangle$ decreases with an increase in the (uniform) valency v of the lattice.

Whereas the N dependence of $\langle n \rangle$ is qualitatively correct for the finite lattices considered in this study, the observation that the lattices diagrammed in Figs. 1–9 are *not* characterized by a uniform valency v limits the usefulness of Eq. (4). In fact, we need to introduce some composite (average) lattice parameters in order to be able to compare trends in the data generated for the variety of lattices considered in this study. Specifically, we need one parameter to account for the nonuniform valency and one parameter to reflect and/or characterize the variety of geometrical shapes. Consistent with the identification of an overall (average) walk length $\langle \bar{n} \rangle$,

TABLE II. Lattice characteristics and stochastic results: Figs. 4–7.

Lattice	N	N_b	$(\bar{r}^2)^{1/2}$	$\langle \bar{n} \rangle$	$\bar{v}$	A
Fig. 4(a)	48	22	2.565 801	91.099 492	4.979	31.177
Fig. 4(b)	48	22	2.576 481	98.892 923	3.458	28.426
Fig. 5(a)	48	24	2.757 565	98.482 040	4.875	30.311
Fig. 5(b)	48	24	2.757 565	101.380 56	3.417	30.311
Fig. 5(c)	48	24	2.857 738	103.240 59	3.417	35.000
Fig. 5(d)	48	24	3.024 208	105.281 53	4.875	30.311
Fig. 6(a)	48	30	2.901 149	116.438 33	3.291	32.000
Fig. 6(b)	48	30	3.685 557	128.675 19	2.625	41.569
Fig. 7(a)	48	34	3.181 981	135.708 86	2.583	38.971
Fig. 7(b)	48	34	3.708 099	154.133 15	2.583	38.971
Fig. 7(c)	48	34	4.681 524	175.763 61	3.166	30.000
"Ladder"	48	48	6.940 221	431.176 47	2.917	23.000

$$\langle \bar{n} \rangle = \frac{\sum_i \langle n \rangle_i}{\sum_i i} , \tag{8}$$

where $\langle n \rangle_i$ is the mean walk length for a trap situated at site i on a given lattice, and the sum is over all lattice sites i, we construct

$$\bar{\nu} = \frac{\sum_i \nu_i}{\sum_i i} , \tag{9}$$

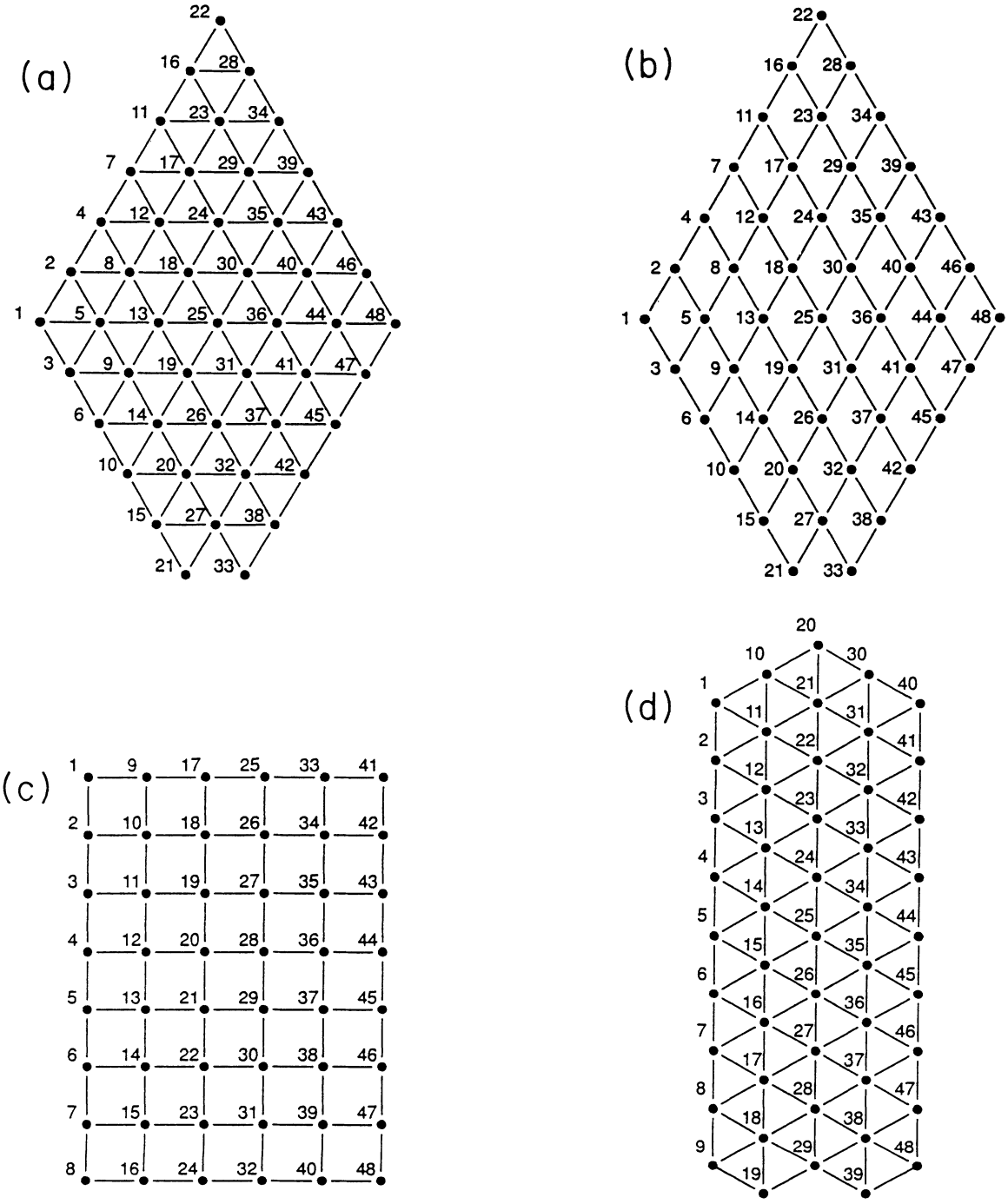

FIG. 5. (a) Lattice characteristics: $\{N, N_b, (\bar{r}^2)^{1/2}, \bar{\nu}\} = \{48, 24, 2.757\,565, 4.875\}$. (b) Lattice characteristics: $\{N, N_b, (\bar{r}^2)^{1/2}, \bar{\nu}\} = \{48, 24, 2.757\,565, 3.417\}$. (c) Lattice characteristics: $\{N, N_b, (\bar{r}^2)^{1/2}, \bar{\nu}\} = \{48, 24, 2.857\,738, 3.417\}$. (d) Lattice characteristics: $\{N, N_b, (\bar{r}^2)^{1/2}, \bar{\nu}\} = \{48, 24, 3.024\,208, 4.875\}$.

where v_i is the valency of site i of the lattice, the sum again being taken over all sites i. To distinguish among the various geometrical shapes of the finite lattices considered here, we construct

$$(\bar{r}^2)^{1/2}=\left[\frac{\sum_i r_i^2}{\sum_i i}\right]^{1/2}, \tag{10}$$

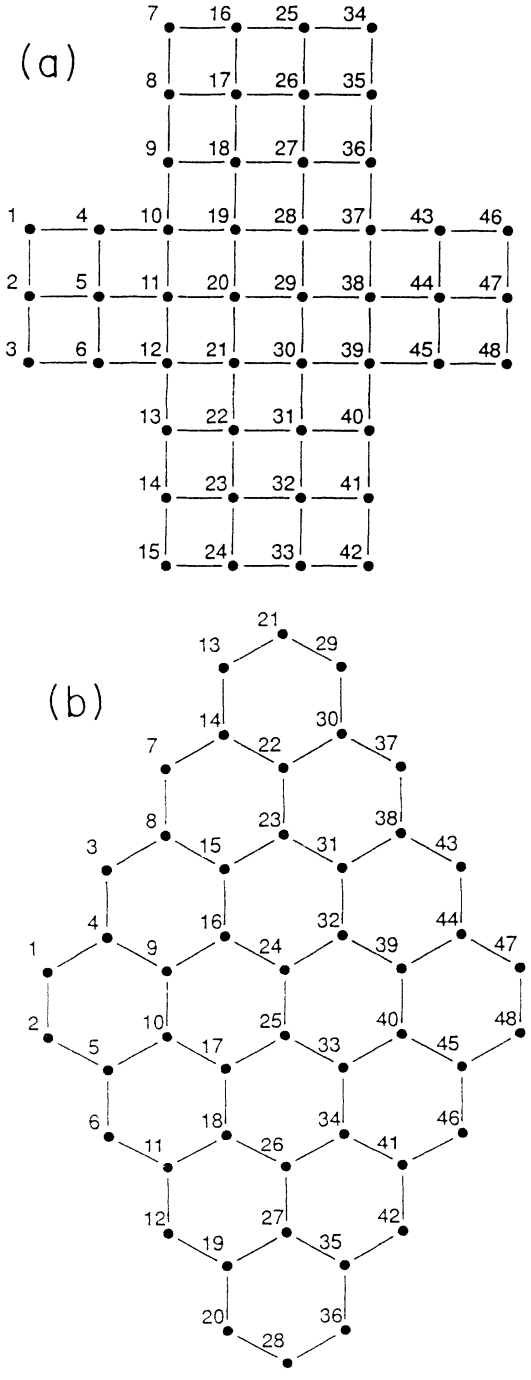

FIG. 6. (a) Lattice characteristics: $\{N,N_b,(\bar{r}^2)^{1/2},\bar{v}\}=\{48,30,2.901\,149,3.291\}$. (b) Lattice characteristics: $\{N,N_b(\bar{r}^2)^{1/2},\bar{v}\}=\{48,30,3.685\,557,2.625\}$.

TABLE III. Lattice characteristics and stochastic results: Figs. 8 and 9.

Lattice	N	N_b	$(\bar{r}^2)^{1/2}$	$\langle\bar{n}\rangle$	$\bar{v}$	A
Fig. 8(a)	48	34	1.651 588	132.792 28	4.458	25.981
Fig. 8(b)	48	34	2.975 595	134.294 19	4.458	25.981
Fig. 8(c)	48	34	3.165 570	137.970 04	4.458	25.981
Fig. 8(d)	48	34	3.230 712	145.592 84	4.458	25.981
Fig. 8(e)	48	34	4.672 615	178.123 32	4.458	25.981
Fig. 9(a)	48	34	3.099 059	134.310 09	3.208	30.000
Fig. 9(b)	48	34	3.158 982	137.018 50	3.208	30.000
Fig. 9(c)	48	34	3.350 995	142.545 92	3.208	30.000
Fig. 9(d)	48	34	3.705 289	151.711 08	3.208	30.000

the root-mean-square distribution of lattice sites with respect to the "center" of a given lattice. For those lattice structures characterized by two (or more) axes of bilateral symmetry, the intersection of these axes is taken as the "center" of the lattice. For lattices with only one axis of bilateral symmetry, we identify a "stochastic center," defined as that lattice point on the bilateral axis for which the calculated $\langle n\rangle_i$ has the minimum value.

From the $\langle n\rangle_i$ data calculated for each of the lattices diagrammed in Figs. 1–9 [6] and from a consideration of their respective geometrical "shapes," we have calculated $\langle\bar{n}\rangle$, $\bar{v}$, and $(\bar{r}^2)^{1/2}$ for each lattice. These values are recorded in Tables I–III, along with the values of N, N_b, and A, where A is the area encompassed by the given figure. These data will be the basis of our subsequent discussion, and will provide the basis for the correlations derived in this study.

Turning first to the data displayed in Table I for the case $N=16$, it is evident that the primary "order parameter" is N_b. Once N_b has been specified, the root-mean-square distance $(\bar{r}^2)^{1/2}$ provides a systematic organization of the data. Then, for a common setting of the $\{N_b,(\bar{r}^2)^{1/2}\}$, the data may be further organized in terms of the average valency $\bar{v}$ of the lattice being considered. In particular, as N_b increases from $N_b=10$ to 12 to 14, the values of $\langle\bar{n}\rangle$ (taken as a group) systematically increase. For $N_b=10$, $\langle\bar{n}\rangle$ increases as $(\bar{r}^2)^{1/2}$ increases (while $\bar{v}$ remains constant); for $N_b=12$, a similar increase of $\langle\bar{n}\rangle$ with $(\bar{r}^2)^{1/2}$ is observed. Notice, however, that for fixed $\{N_b=12,(\bar{r}^2)^{1/2}=1.581\,139\}$, $\langle\bar{n}\rangle$ increases with respect to a decrease in the average valency $\bar{v}$. Thus, for fixed $\{N_b,(\bar{r}^2)^{1/2}\}$, the qualitative dependence of the average walk length $\langle\bar{n}\rangle$ on the valency (here, $\bar{v}$) is the same as that predicted by Eq. (4), the latter result proved for nearest-neighbor random walks on infinite periodic lattices. Finally, examination of Figs. 2(c) and 2(d) and the corresponding data in Table I reveals that for fixed $\{N,N_b,(\bar{r}^2)^{1/2},\bar{v}\}$, the value of $\langle\bar{n}\rangle$ remains constant, despite the fact that the shape of the lattice "looks" different. This last case reflects the fact that finite lattices subject to a diffeomorphic transformation leave invariant the value of $\langle\bar{n}\rangle$. Since $\langle\bar{n}\rangle$ summarizes the net result of considering all possible flows initiated from all possible sites (i.e., "initial conditions") on the lattice, $\langle n\rangle$ is playing the role of a topological invariant for the class of

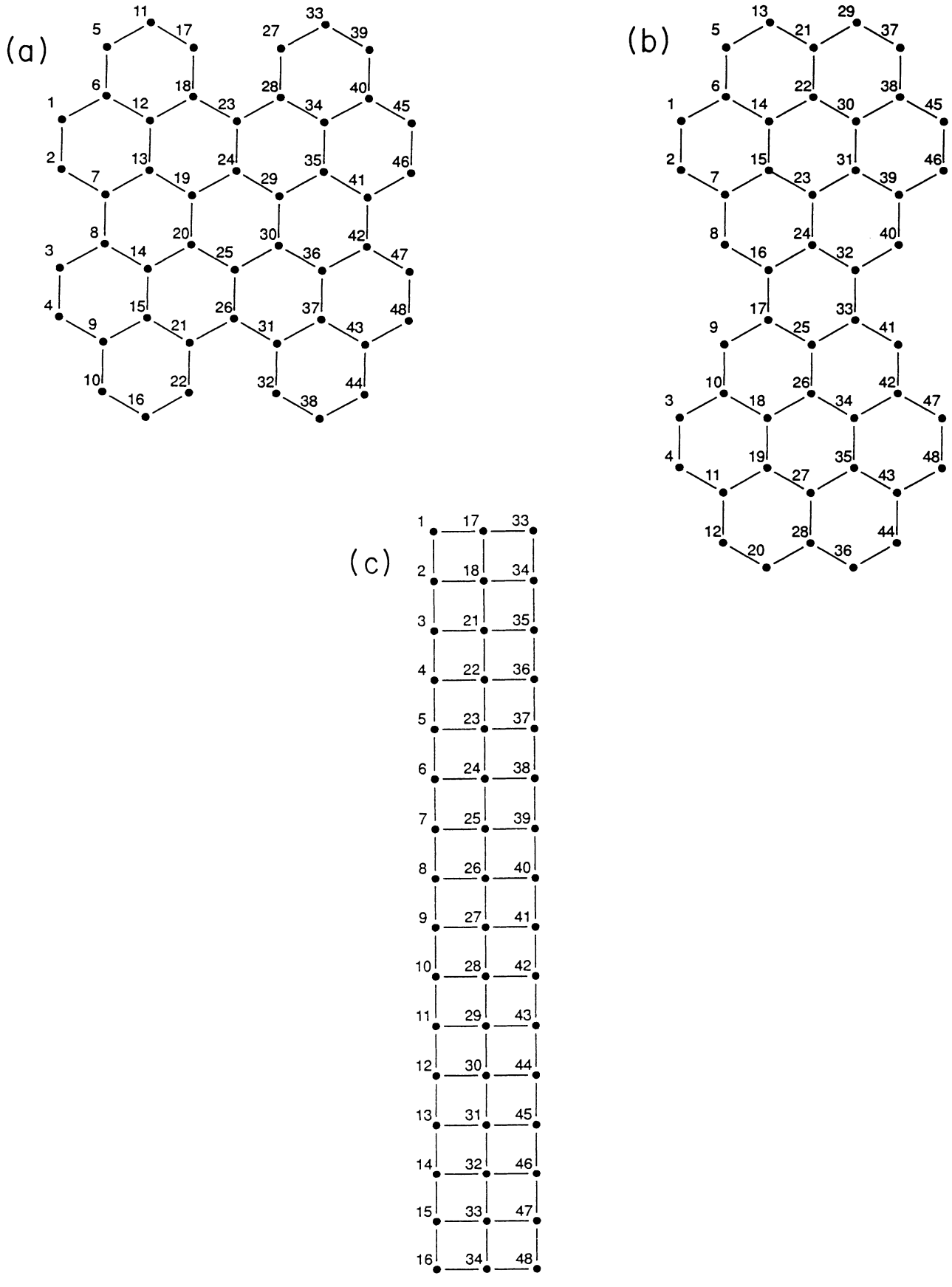

FIG. 7. (a) Lattice characteristics: $\{N_b(\bar{r}^2)^{1/2},\bar{v}\} = \{48,34,3.181\,981,2.583\}$. (b) Lattice characteristics: $\{N,N_b(\bar{r}^2)^{1/2},\bar{v}\} = \{48,34,3.708\,099,2.583\}$. (c) Lattice characteristics: $\{N,N_b,(\bar{r}^2)^{1/2},\bar{v}\} = \{48,34,4.681\,524,3.166\}$.

problems studied here.

The conclusions noted above for the case $N=16$ are sustained if one considers the more complex structures diagrammed in Figs. 4–7 and the $(N,N_b)=(48,48)$ "ladder" diagram (not displayed). Generally speaking, $\langle \bar{n} \rangle$ increases with increasing N_b; once (N,N_b) are set, $\langle \bar{n} \rangle$ increases with increasing $(\bar{r}^2)^{1/2}$; and, once $\{N,N_b,(\bar{r}^2)^{1/2}\}$ are set, $\langle \bar{n} \rangle$ increases with decreasing $\bar{v}$ [compare Figs. 5(a) and 5(b) and the corresponding data in Table II).] That $\bar{v}$ does *not* take precedence over $(\bar{r}^2)^{1/2}$ as an organizing parameter for $\langle \bar{n} \rangle$ can be seen in several cases, e.g., the lattices [Figs. 5(c) and 5(d)], where $\bar{v}=3.417$ in the former case and $\bar{v}=4.875$ in the latter figure, with the corresponding $\langle \bar{n} \rangle$ values increasing

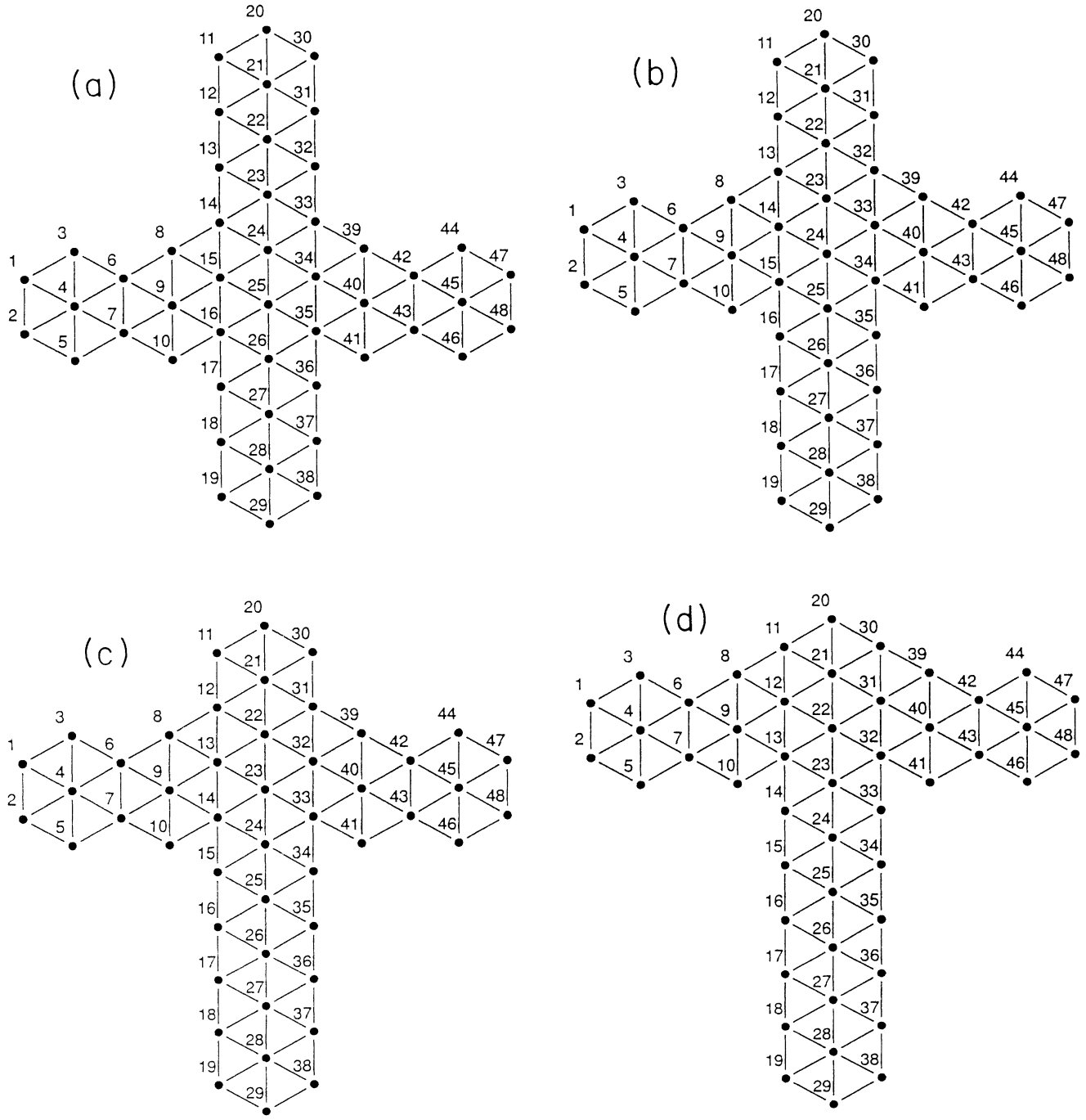

FIG. 8. (a) Lattice characteristics: $\{N,N_b,(\bar{r}^2)^{1/2},\bar{v}\}=\{48,34,1.651\,588,4.458\}$. (b) Lattice characteristics: $\{N,N_b,(\bar{r}^2)^{1/2},\bar{v}\}=\{48,34,2.975\,595,4.458\}$. (c) Lattice characteristics: $\{N,N_b,(\bar{r}^2)^{1/2},\bar{v}\}=\{48,34,3.165\,570,4.458\}$. (d) Lattice characteristics: $\{N,N_b,(\bar{r}^2)^{1/2},\bar{v}\}=\{48,34,3.230\,712,4.458\}$. (e) Lattice characteristics: $\{N,N_b,(\bar{r}^2)^{1/2},\bar{v}\}=\{48,34,4.672\,615,4.458\}$.

with an *increase* in the value of $\bar{v}$. See also Figs. 7(b) and 7(c).

Finally, consider the more structured lattices displayed in Figs. 8 and 9, together with the data presented in Table III. Within each of the individual series, Figs. 8 and 9, it is seen that, consistent with our previous discussion, for fixed $(N,N_b)=(48,34)$, the $\langle \bar{n} \rangle$ values calculated increase with increasing values of $(\bar{r}^2)^{1/2}$. In fact, an even more striking correlation can be seen. Notice first that all of the lattices diagrammed in Figs. 8 and 9 are characterized by a single axis of bilateral symmetry; in contrast, the $(N,N_b)=(48,34)$ lattices displayed in Figs. 7 have two, mutually perpendicular axes of bilateral symmetry. Except for the single inversion in the data for Figs. 8(d) and 9(c), the $\langle \bar{n} \rangle$ values calculated for all lattices within a given symmetry class once again increase with increasing values of the root-mean-square distance $(\bar{r}^2)^{1/2}$.

IV. CONCLUSIONS

In this section, we contrast and distinguish the results obtained here for $(d=2)$-dimensional nearest-neighbor walks on finite lattices with those derived from studies of random walks on periodic lattices of unit cells. With respect to the latter class of problems, we shall rely not only on earlier analytical work [1,2], but also on numerically exact results obtained using the theory of finite Markov processes when applied to walks on hexagonal [3(b)] ($\nu=3$), square-planar [9] ($\nu=4$), and triangular [8] ($\nu=6$) lattices.

First of all, as noted earlier, from Montroll's results for periodic lattices [see Eq. (4)], it is known that $\langle n \rangle$ increases with increasing N. Our results on finite lattices support this conclusion. Moreover, our studies on finite lattices also show that $\langle \bar{n} \rangle$ generally increases with increasing N_b. The only case uncovered for which there

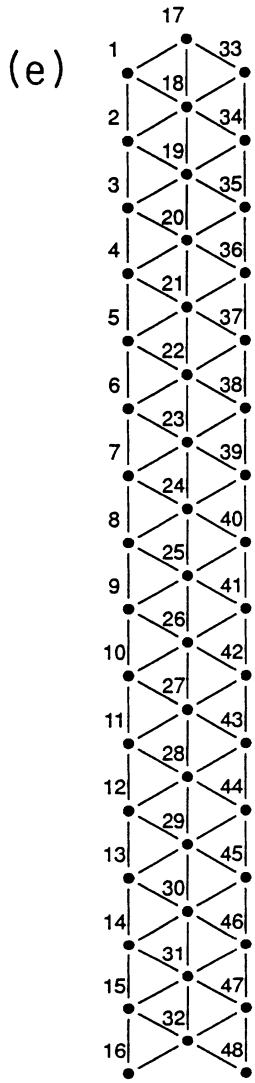

FIG. 8. (*Continued*).

was an "inversion" in order with respect to the dependence on N_b was Fig. 4(b) vs Fig. 5(a); in the former lattice, $\{N_b,\bar{\nu}\}=\{22,3.458\}$, whereas in the latter one $\{N_b,\bar{\nu}\}=\{24,4.875\}$, and it is probable that the higher connectivity of the lattice, Fig. 5(a), may account for the slight differences in $\langle \bar{n} \rangle$ values: $\langle \bar{n} \rangle = 98.892\,923$ [Fig. 4(b)] vs $\langle \bar{n} \rangle = 98.482\,040$ [Fig. 5(a)], a difference of less than 0.5%.

It is in the dependence of $\langle \bar{n} \rangle$ on the (average) valency $\bar{\nu}$ that the results obtained here stand in greatest contrast to the analytic and numerical results obtained for periodic lattices. Once again, from earlier studies on periodic lattices, it is anticipated that $\langle \bar{n} \rangle$ should decrease systematically with increase in the (uniform) valence ν of the lattice [again, see Eq. (4) and Eqs. (5)–(7)]. In fact, this result pertains as well to random walks on $(d=3)$-dimensional periodic lattices of unit cells [9,10] and can also be demonstrated analytically and numerically for

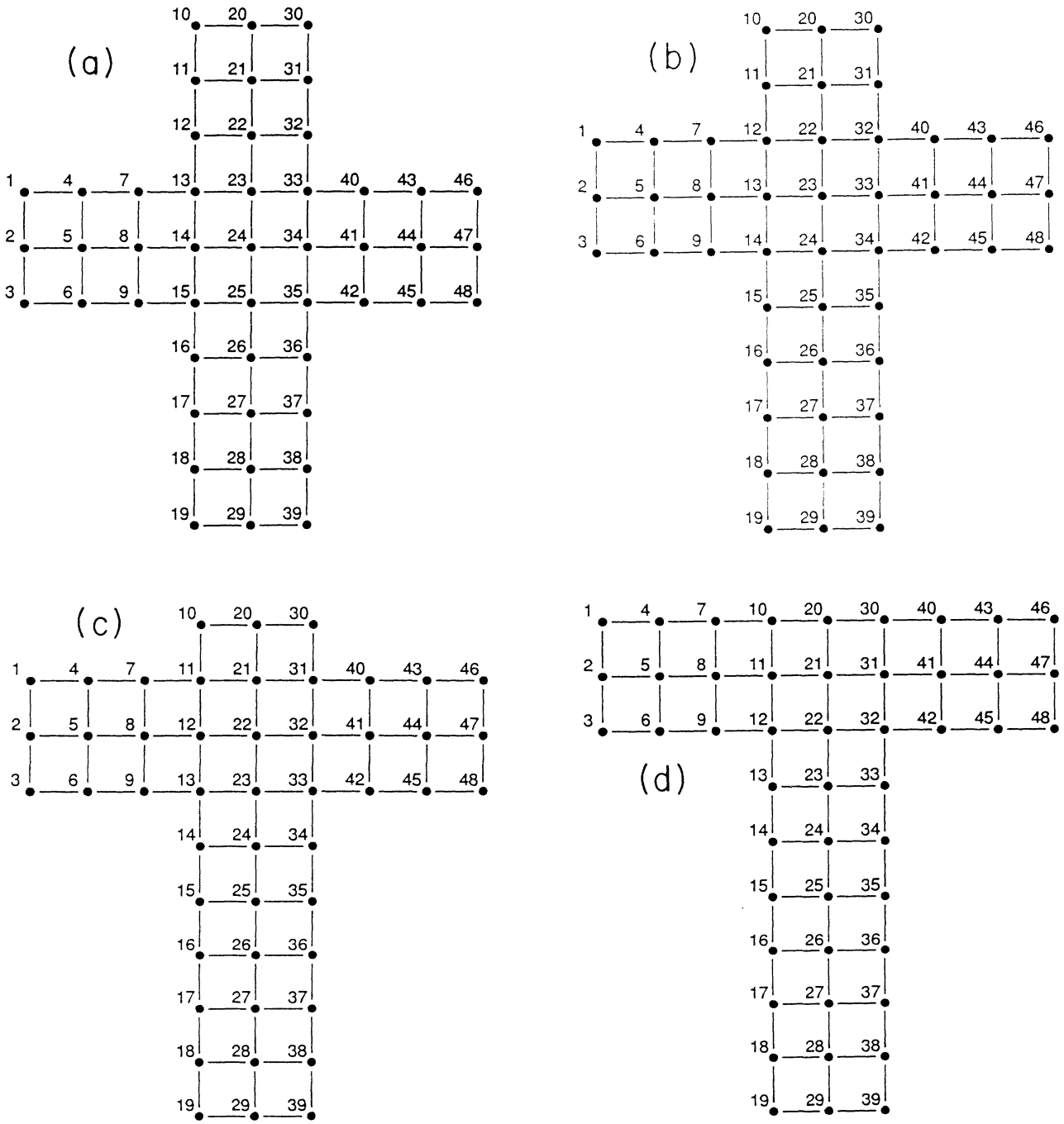

FIG. 9. (a) Lattice characteristics: $\{N,N_b,(\bar{r}^2)^{1/2},\bar{\nu}\}=\{48,34,3.099\,059,3.208\}$. (b) Lattice characteristics: $\{N,N_b,(\bar{r}^2)^{1/2},\bar{\nu}\}=\{48,34,3.158\,982,3.208\}$. (c) Lattice characteristics: $\{N,N_b,(\bar{r}^2)^{1/2},\bar{\nu}\}=\{48,34,3.350\,995,3.208\}$. (d) Lattice characteristics: $\{N,N_b,(\bar{r}^2)^{1/2},\bar{\nu}\}=\{48,34,3.705\,289,3.208\}$.

walks on higher-dimensional ($d \leq 8$) cubic lattices [11,3(c)]. In the latter problem, $\nu = 2d$ and hence the higher the dimensionality of the space, the greater the number of pathways to a centrally located deep trap in a periodic array of (cubic) unit cells; in fact, the decrease in $\langle n \rangle$ is found to be quite dramatic with increase in the dimensionality d, and hence ν. On the other hand, it should also be recognized that an increase in ν will result in a greater number of pathways that allow the random walker to move *away* from the trap. For periodic lattices, this latter option simply positions the random walker close to the trap in an adjacent unit cell. It is evident therefore why the strong ν dependence seen for periodic lattices is weakened when one studies the same class of nearest-neighbor random-walk problems on the finite lattice systems considered here: for finite lattices, moving away from the trap does not position the random walker closer to a trap in a neighboring unit cell; it positions the walker closer to the finite boundary of the lattice from whence it must (eventually) work itself back.

The discussion presented in Sec. IV leads to the conclusion that the root-mean-square distance $(\bar{r}^2)^{1/2}$, calculated with respect to the "center" of the finite lattice, is a parameter second in importance only to $\{N, N_b\}$ in organizing the data on $\langle n \rangle$. A further, concrete illustration of this conclusion is provided by considering in more detail the Penrose decagons diagrammed in Fig. 1 and the larger Penrose platelet shown in Fig. 4(a). As is evident, the latter figure may be constructed by a superposition of the simpler structures I, II, and III, and IV. Notice that, as labeled, the figures I and II are "optical isomers," as are figures III and IV. No differences in the $\langle \bar{n} \rangle$ values calculated for the structures I and II are found (nor are the $\langle \bar{n} \rangle$ values for III and IV different); however, the $\langle \bar{n} \rangle$ values for I (II) *are* different from those for III (IV). The only lattice characteristic that distinguishes I (II) from III (IV) is the value of $(\bar{r}^2)^{1/2}$, the values of $\bar{\nu}$ and A being exactly the same (see Table I). With respect to the calculation of $(\bar{r}^2)^{1/2}$ in these two cases, whereas the "geometric center" and the "stochastic center" for the figure I (II) coincide, the two "centers" are different for III (IV), a consequence of the fact that III (IV) has only a single axis of bilateral symmetry. Once the importance of choosing the "stochastic center" in calculating $(\bar{r}^2)^{1/2}$ for finite lattices with a single axis of bilateral symmetry is understood, the results calculated for the structures I (II) and III (IV), as well as the results for the full range of structures displayed in Figs. 1–8, fall into place.

A further interesting feature of the four $N = 16$ Penrose decagons is that, for $N = 16$, the value of N_b is smaller than any other "regular" lattice that we have been able to construct (see Figs. 2 and 3) subject to the constraint that the "bond length" connecting all lattice points be fixed. (Recall that we set the metric for all lattices at $l = 1$.) Given that the $\langle \bar{n} \rangle$ values calculated for the $N = 16$ Penrose decagons are smaller than the $\langle \bar{n} \rangle$ values for the other $N = 16$ lattices diagrammed in Figs. 2 and 3 points again to the importance of N_b as a principal organizing parameter for the class of random walk problems studied here. When lattices $N = 48$ are considered, however, it is possible to construct a (triangular) lattice [Fig. 4(a)] with the same number $N_b = 22$ of boundary sites as the Penrose platelet [Fig. 4(b)]. In this case, $(\bar{r}^2)^{1/2}$ is smaller for the lattice diagrammed in Fig. 4(a), with the consequence that the overall $\langle \bar{n} \rangle$ is smaller for the more compact "triangular" lattice. Finally, a distinguishing feature of the Penrose platelet diagrammed in Fig. 4(a) is the presence of one site of valency $\nu = 7$; positioning a trap at that site leads to the smallest site-specific value of $\langle \bar{n} \rangle (= 36.212\,847)$ for all lattices with $N = 48$.

In the preceding section, we noted that finite lattices subject to a metric-preserving, diffeomorphic transformation leave invariant the value of $\langle \bar{n} \rangle$; recall the results obtained for Figs. 2(c) and 2(d). From the results obtained in studying the *labeled* Penrose decagons I and II (or III and IV), lattice pairs which are "optical isomers" of each other, we also find that the number $\langle \bar{n} \rangle$ plays the role of a topological invariant. Finally, we note that $\langle \bar{n} \rangle$ is invariant when computed for random walks on the finite strip, Fig. 7(c), when that lattice is subject to the following two operations: (1) joining the sites 1,16; 17,34; 33,48; and (2) joining the sites 1,48; 17,34; 33,16. That is, the $\langle \bar{n} \rangle$ values calculated for random walks on a "ring" versus walks on a Moebius strip are identical. The common feature in each of these cases is that calculation of $\langle \bar{n} \rangle$ does not allow one to discriminate between certain pairs of finite lattice structures [Fig. 2(c) vs Fig. 2(d); I vs II (or III vs IV) in Fig. 1; the "ring" versus the Moebius strip generated from Fig. 7(c)]. It is interesting to consider what constraint on the motion of the random walker would have to be relaxed in order that different values of $\langle \bar{n} \rangle$ would result in each of the cases noted. Two "symmetry-breaking" possibilities that will be pursued in our subsequent work are (1) allowing non-nearest-neighbor transitions of the random walker between sites on the lattice, and (2) considering the presence of downrange potential interactions between the random walker and the stationary target (trap). While the flows would still be ergodic, both generalizations would allow the random walker to sample a larger fraction of the surface (accessible phase space) in its site-to-site displacements, and may result in discrimination between the pairs of lattice structures considered.

Finally, it is of interest to speculate on the possible relevance of our study and attendant conclusions to a process of morphogenesis. For definiteness, consider the composite set of data for the case $N = 48$ (see Tables II and III). Generally speaking, the lattice structures characterized by the smaller values of N_b are more compact. The more articulated structures can be thought of as being generated by transposing *interior* lattice points to the *boundary* of the figure. Suppose that this process is induced by a molecule diffusing in $(d = 3)$-dimensional space, impinging on the surface, diffusing randomly on that surface in a series of nearest-neighbor displacements, and then triggering a geometrical transformation of the lattice, i.e., an increase $N_b \rightarrow N_b'$ with $N_b' > N_b$. [Recall that the values calculated for $\langle \bar{n} \rangle$ reflect all possible initial conditions (i.e., initialization points in the particle's trajectory) and all possible nearest-neighbor trajectories to the target or receptor site.] One can then envision a

further "unfolding" of the initial structure, $N_b \rightarrow N_b' \rightarrow N_b''$ (with $N_b'' > N_b' > N_b$), triggered by a similar process of surface-mediated walks of an "activator" molecule to a "receptor" site (molecule). If one is seeking an "order parameter" for this series of transformations, one that ensures that the underlying reaction efficiency of the process at each stage be maximized (i.e., that $\langle \bar{n} \rangle$ be minimized), our studies show that parameter would be $(\bar{r}^2)^{1/2}$. In other words, if one demands that the efficiency of the morphogenetic process be optimized as the original structure "unfolds," one would select those new structures characterized by settings of $N_b, N_b', N_b'', \ldots$ for which $(\bar{r}^2)^{1/2}$ is minimized.

Two specific examples can be given here. First, in the set of possible structures evolving from the $(N, N_b) = (48, 24)$ lattice, Fig. 6(a), via a signal-processing event of the type described above, the $(N, N_b) = (48, 34)$ lattice, Fig. 9(a), would be the preferred structure, rather than the options in Figs. 9(b), 9(c), or 9(d). Second, any of the articulated $(N, N_b) = (48, 34)$ lattices, Figs. 8(a)–8(d), evolving from the $(N, N_b) = (48, 24)$ lattice, Fig. 5(a), would be preferred to the "linear" $(N, N_b) = (48, 34)$ lattice, Fig. 8(e), if morphogenesis is guided by the order parameter $(\bar{r}^2)^{1/2}$. It is this observation, arising from an analysis of the lattice-statistical data presented in this paper, which we believe may have relevance to the morphogenetic problem of predicting the optimal design (here, shape) of finite, planar arrays having physical or chemical receptors.

ACKNOWLEDGMENTS

The authors would like to thank Mr. Kevin Hsieh for assistance in performing some of the calculations reported in this paper.

[1] G. H. Weiss and R. J. Rubin, Adv. Chem. Phys. **52**, 363 (1983).

[2] (a) E. W. Montroll, Proc. Symp. Appl. Math. Am. Math. Soc. **16**, 193 (1964); (b) E. W. Montroll and G. H. Weiss, J. Math. Phys. **6**, 167 (1965); (c) E. W. Montroll, *ibid.* **10**, 753 (1969).

[3] See, for example, (a) C. A. Walsh and J. J. Kozak, Phys. Rev. Lett. **47**, 1500 (1981); (b) P. A. Politowicz and J. J. Kozak, Phys. Rev. B **28**, 5549 (1983); (c) J. J. Kozak, Phys. Rev. A **44**, 3519 (1991).

[4] For a general discussion, see (a) E. W. Montroll and K. E. Shuler, Adv. Chem. Phys. **1**, 361 (1958); (b) G. Nicolis and I. Prigogine, *Self-Organization in Nonequilibrium Systems* (Wiley, New York, 1977); (c) H. Haken, *Synergetics* (Springer-Verlag, Heidelberg, 1977).

[5] Discussion of this relationship for lattice systems is presented in (a) L. G. Boulu and J. J. Kozak, Mol. Phys. **62**, 1449 (1987); (b) **65**, 193 (1988); (c) P. A. Politowicz, R. A. Garza-López, D. E. Hurtubise, and J. J. Kozak, J. Phys. Chem. **93**, 3728 (1989).

[6] The complete set of $\langle n \rangle_i$ for the lattices diagrammed in Figs. 1–9 is available from the authors upon request.

[7] W. Th. F. den Hollander and P. W. Kasteleyn, Physica A **112**, 523 (1982).

[8] P. A. Politowicz and J. J. Kozak, Langmuir **4**, 305 (1988).

[9] C. A. Walsh and J. J. Kozak, Phys. Rev. B **26**, 4166 (1982).

[10] P. A. Politowicz and J. J. Kozak, Mol. Phys. **62**, 939 (1987).

[11] P. A. Politowicz, J. J. Kozak, and G. H. Weiss, Chem. Phys. Lett. **120**, 388 (1985).